Construction and Building Materials 337 (2022) 127615

Contents lists available at ScienceDirect

Construction and Building Materials

journal homepage: www.elsevier.com/locate/conbuildmat

The influence of using wet cellulose poultice on nanolime consolidation treatments applied on a limestone

J.S. Pozo-Antonio [a,*], J. Otero [b], N. González [a]

[a] CINTECX, GESSMin Group, Departamento de Enxeñaría dos Recursos Naturais e Medio ambiente, Universidade de Vigo, 36310 Vigo, Spain
[b] Departamento de Mineralogía y Petrología, Universidad de Granada, Fuentenueva s/n, 18002 Granada, Spain

ARTICLE INFO

Keywords:
Consolidant
Carbonate stone
Nanolime
Stone deterioration
Physical property
Isopropanol
Poultice

ABSTRACT

Consolidation treatment with nanolime is a common conservation intervention which needs more research to enhance penetration and mechanical properties while also minimizing the undesired white veil on the surface which significantly alters the surface appearance. In this light, the application of a cellulose poultice soaked in distilled water over the treated surface with nanolime tries to prevent the formation of white hazes and to favour nanolime carbonation and penetration in the pore structure. However, the real influence of this practice on the consolidation effectiveness has never been studied yet and is not yet well understood. In order to provide more insights about its most suitable application method, in this study, we investigated the effectiveness of a wet cellulose poultice for two different nanolime consolidation treatments on a weathered limestone. Nanolime has been synthetized by anion exchange processes and dispersed in two mediums: i) water and ii) 50% v/v of water and alcohol. The influence of the poultice on the penetration and aesthetic properties has been studied by drilling resistance measurement, ultrasounds test, stereomicroscopy, measurements of roughness and static contact angle, spectrophotometry and scanning electron microscopy (superficial and cross sectioned samples). Additionally, consolidation effectiveness has been evaluated through the changes in apparent density, open porosity, porosity network in the outer 5 mm of the surface by mercury intrusion porosimetry and surface cohesion by the peeling test. Results show that, contrary to what is usually assumed, samples where a wet cellulose poultice was applied after the consolidant reached the lowest penetration levels and retained lower dry matter in comparison to their counterparts without poultice. A consolidation treatment with nanolime is more complex that it is generally considered, and the application of poultices is not always enhancing consolidation level; the most suitable application procedure must be chosen with regards to the nanolime and substrate specific characteristics.

1. Introduction

Heritage structures built with stones can be subjected to natural deterioration agents, such as precipitation, solar radiation, wind, etc. and consequently, different alteration processes (dissolution, oxidation, crystallization of soluble salts, etc.) can occur [1]. The resulting deterioration forms (e.g. chromatic changes, disintegration, delamination, erosion, efflorescences, etc.) depend on the intrinsic properties of the stone (texture and porosity, chemical and mineralogical composition, etc.) [2–6]. Other important deterioration agents are those related to anthropogenic activity such as atmospheric pollution and vandalism (mechanical damage, application of paints, graffiti, etc.) [6,7] which have accelerated the deterioration of these stones [8,9]. Following [7,10], the detachment deterioration patterns include blistering, bursting, delamination, disintegration (crumbling and granular disintegration), fragmentation (splintering and chipping), peeling and scaling (flaking and contour scaling), which are also linked to some other structural failures or the crystallization of soluble salts.

Considering the artistic, historical and economic importance of the tangible cultural heritage of a country, a correct conservation requires research, in order to avoid any risk to the artistic and historical value of the structure. Consolidation is a process consisting of the impregnation of the deteriorated stone with chemical products (i.e. consolidants) in order to strengthen the stone surfaces and to mitigate the disintegration process and consequently re-establish the cohesion and the mechanical resistance [11,12]. The composition of the consolidants has undergone

* Corresponding author.
E-mail address: ipozo@uvigo.es (J.S. Pozo-Antonio).

https://doi.org/10.1016/j.conbuildmat.2022.127615
Received 1 November 2021; Received in revised form 9 March 2022; Accepted 20 April 2022
Available online 27 April 2022

an intense evolution over time. From the Ancient Greece to the middle of the 20th century, the conservation of carbonate stones belonging to European buildings has been carried out mainly through the application of lime-water with a good chemical compatibility with the substrate. Lime-water consists of a saturated solution of calcium hydroxide ($Ca(OH)_2$) in water, which after reacting with carbon dioxide (CO_2) produced calcite ($CaCO_3$) with low solubility in water [13]. However, this technique has some limitations such as the low penetration of the lime-water through the pores and fissures of the stone as consequence of the low carbonation ratio and especially the low solubility of calcium hydroxide in water makes this process sometimes requires many applications [14,15]. In order to improve its performance, an excess of $Ca(OH)_2$ can be used, thus obtaining a suspension with a greater quantity of calcium hydroxide particles for an equal consumption of solution. Due to the milky appearance as consequence of this $Ca(OH)_2$ excess, this consolidant is known as lime-milk [16].

In the middle of the 20th century, new commercial consolidants appeared, such as tetraethyl orthosilicate (TEOS), which is an alkoxysilane, or trimethoxymethylsilanes (MTMOS), which are alkyl alkoxysilanes, and which are also products created specifically for the consolidation of silicate stones [17–19]. These new products show an unsatisfactory chemical compatibility with carbonate stones due to the different chemical composition which is different from that of the carbonate nature of the stones and the silicate matrix created by the consolidant, which can lead to failing consolidation treatments [1,20]. Therefore, the lack of an effective consolidation product for carbonate stones persisted throughout the second half of the 20th century. At the beginning of the 21st century, nanotechnology was used to provide consolidants for carbonate stones. The use of calcium hydroxide particles much smaller than those used to date was considered to be an improvement. Specifically, the fact that the nanoparticles are smaller than 100 nm allows them to have a greater specific surface area, and then, their reactivity is higher than regular size particles [16,21–28].

Nanolime ($Ca(OH)_2$ nanoparticles) represents an improvement with respect to the limiting aspects that affected the traditional lime-water method [25,29,30]. The nanolime has the same high chemical compatibility with the carbonate stone while also, in addition, nanoparticles have a faster carbonation process [26] and consequently the obtained particles have a reduced size and better penetration into the stone [27].

Nanolime is commonly synthesized by various routes [16] leading to nanoparticles that are dispersed in alcohol (mostly isopropanol or ethanol). However, recently, a new method has been developed that is based on synthesizing lime nanoparticles following anion exchange processes [31–33] that allow the synthesis of nanoparticles directly in water from a fast method, which saves energy and is respectful with the environment. Furthermore, according to this patent, the resulting nanoparticles have a smaller particle size and faster carbonation compared to the other synthesis routes. This nanolime solution is commonly found in a water-based system, but several authors reported that the addition of nanolime particles to alcoholic solutions promotes a faster carbonation process, which can be also improved with the application of high relative humidity on values above 65% RH [34,35]. In this sense, products such as ethanol, n-propanol or isopropanol could be used to improve the penetration of the nanoconsolidant into the stone and to avoid the consolidant accumulation on the treated surface, which can prevent the penetration of the consolidant and also slow down the flow of water from inside the stone to the outside [36]. However, water + alcohol-based nanolime solutions still raise doubts about their ability to consolidate in depth. In fact, some authors consider that nanolime accumulates just below the surface, due to the rapid evaporation of the solvents used, which could transport the nanoparticles back to the surface during the evaporation process [37–39]. In addition, a surface layer or veil is usually created preventing the consolidant penetration into the stone in the following applications [36,39,40]. In this light, the application of a cellulose poultice soaked in distilled water over the treated surface immediately after the nanolime treatment is a general assumed practice to prevent the formation of white hazes and to favour nanolime carbonation and penetration in the pore structure, which is also recommended in the technical datasheet of nanolime commercial products, i.e., Nanorestore and Calosil, [41,42]. However, the real influence of the poultices on the consolidation effectiveness has never been studied. On the contrary, although several successful treatments have been reported with nanolime [20,25–35,40,43–44], especially more effective than lime-water or milk-lime, the most suitable application procedure for a nanolime treatment, requires more research especially regarding the penetration, surface cohesion and the side-effects on the surfaces.

In this research, in order to provide better insights about its most suitable application method, we investigated the influence of a wet cellulose poultice straight after two nanolime consolidation treatments on a weathered limestone. For this purpose, nanolime has been synthetized in the laboratory by anion exchange processes and dispersed in two mediums: i) water and ii) 50% v/v of water and alcohol. The influence of these poultices in the penetration and aesthetic properties has been studied by the drilling resistance measurement system (DRMS), the P wave velocity (vp) measurement by ultrasounds test, stereomicroscopy, measurement of roughness and static contact angle, colour spectrophotometry and scanning electron microscopy using superficial and cross sectioned samples. Additionally, the consolidation effectiveness of treatments has been also evaluated through the observation of changes in apparent density, open porosity, porosity network in the outer 5 mm of the surface by mercury intrusion porosimetry and (MIP) and surface cohesion by the peeling tes.t.

2. Materials and methods

2.1. Stone

A limestone (Fig. 1a) covered with a black crust was obtained from the Building Research Establishment (UK) outdoor historic stone deposit. This stone was also used in previous studies where it is included a full characterisation of the stone is included [43]. It is a sedimentary rock composed of ooids cemented by sparry calcite (Fig. 1b, d-f) composed mainly of calcite (detected by x-ray diffraction-XRD-, n = 3). It shows an apparent density of 2.13 (±0.03, n = 3) g/cm^3 in accordance to [47] and 2.56 (±0.01, n = 3) g/cm^3 by mercury intrusion porosimeter (MIP) and an open porosity of 19.94 (±0.43, n = 3) % in accordance to [47] and 27.43 (±0.30) % by MIP (Table 1). It presents higher population of pores with diameter between 10 and 50 μm [43]. The piece was cut with a diamond disc cutter in order to obtain 21 cubes with 35 × 35 × 35 mm as dimensions (Fig. 1c).

2.2. Nanolime

Nanolime was synthesized through a patented process based on ion exchanges processes [31–33,44]. During the synthesis, an anion exchange resin (Dowex Monosphere 550A OH by Dow Chemical) is added to an aqueous calcium chloride solution ($CaCl_2$ by Sigma-Aldrich) and nanoparticles are formed by chemical precipitation during the ion exchange process [31]. Following the synthesis, the nanolime was prepared at 5 g/L in water solution. These synthesized nanoparticles are characterized as plate-like hexagonal $Ca(OH)_2$ nanoparticles regularly shaped with a particle size ranging from 20 to 80 nm, which are highly reactive being transformed in pure well-crystalline calcite after only 1 h of air exposure at 65% RH [33]. Two bottles (1L each) were obtained and kept in a refrigerator (5 °C) to mitigate the Ca-alkoxide conversion to increase their effectiveness [45]. In one of the two bottles, after 48 h to achieve the decantation of the nanoparticles, the half of the solvent was extracted with a pipette and then, the same volume was refilled with isopropanol (C_3H_8O) for the 50%-50% W/A solution maintaining the same concentration of 5 g/L. Different ratios have been studied in the past but 50%-50% W/A solution delivered higher carbonation kinetics

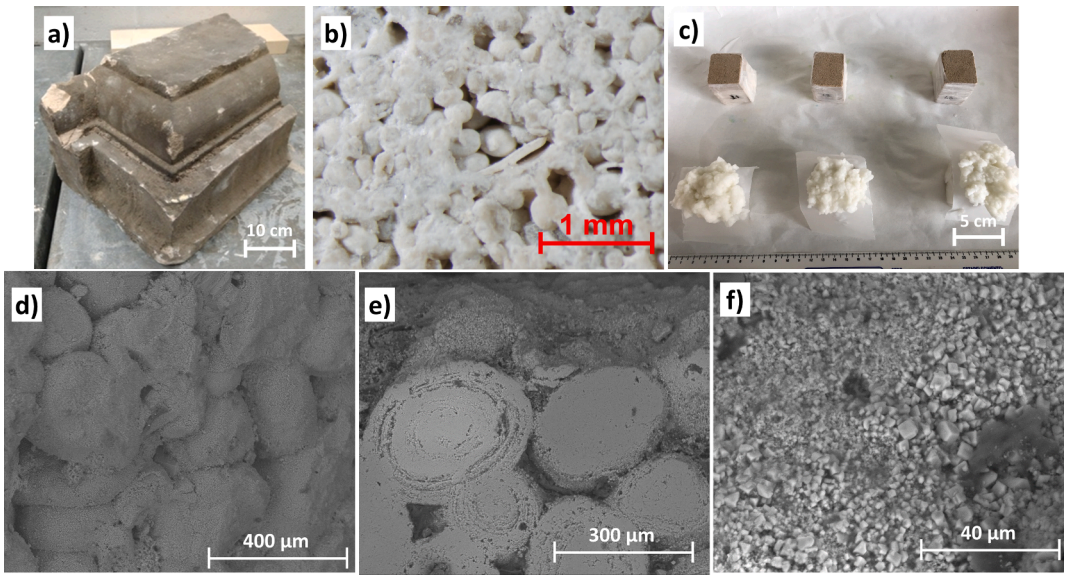

Fig. 1. a) Limestone from the Building Research Establishment (UK) with a black crust. b) Micrographs by stereomicroscope of the limestone. c) samples used in this research: the upper line corresponds to the samples impregnated with water-based nanolime (L) by brush and the bottom line corresponds to the samples impregnated with water-based nanolime and covered immediately by wet cellulose poultice (LP). d–f) Micrographs taken with scanning electron microscopy of the unconsolidated stone after being cut to remove the black crust (S): d) surface and e, f) cross section.

Table 1
Consolidant uptake after each application (g), total uptake (g), content of dry matter (g) and retained matter (% w/w). Moreover, apparent density (kg/m^3) and open porosity (%) of the entire samples in accordance with [47] and those by MIP at samples of the outermost 5 mm are shown. S: unconsolidated stone, L: stone with water-based nanolime, LP: stone with water-based nanolime and poultice, LI: stone with water + isopropanol- based nanolime, LIP: stone with water + isopropanol- based nanolime and poultice.

Sample	Uptake 1st appl. (g)	Uptake 2nd appl. (g)	Uptake 3rd appl. (g)	Total uptake (g)	Dry matter (g)	Retained matter (%)	Apparent density (kg/m^3) [47]	Open porosity (%) [47]	Apparent (skeletal) density (kg/m^3) at MIP superficial 5 mm	Open porosity (%) at MIP superficial 5 mm
S							2128.23 ± 28.46	19.94 ± 0.43	2556.40 ± 11.20	27.43 ± 0.30
L1	1.38	1.15	0.86	3.63 ± 0.29	0.03 ± 0.01	0.80 ± 0.09	2106.58 ± 11.20	20.11 ± 0.42	2509.40 ± 7.95	21.83 ± 0.42
L2	1.44	1.39	0.77							
L3	1.53	1.56	0.87							
LP1	1.37	3.17	0.49	5.01 ± 0.12	0.02 ± 0.01	0.39 ± 0.25	2106.52 ± 1.56	20.04 ± 0.49	2647.60 ± 11.48	22.87 ± 0.34
LP2	1.00	3.45	0.42							
LP3	1.33	3.33	0.46							
LI1	0.91	0.79	0.36	2.54 ± 0.39	0.03 ± 0.01	1.16 ± 0.13	2118.41 ± 15.21	19.54 ± 0.62	2562.50 ± 8.18	23.03 ± 0.35
LI2	1.44	0.92	0.54							
LI3	1.20	0.98	0.44							
LIP1	1.31	0.85	0.44	2.48 ± 0.14	0.02 ± 0.01	1.16 ± 0.06	2107.27 ± 8.24	20.30 ± 0.54	2874.20 ± 10.10	23.69 ± 0.34
LIP2	1.15	0.80	0.38							
LIP3	0.85	0.85	0.49							

in terms of faster transformation of portlandite to pure calcite crystals, improved properties of nanoparticles mitigating the agglomeration (compared to water) and consolidation effectiveness [33].

Two nanolime products were obtained: i) nanolime particles dispersed in water in 5 g/L; and ii) nanolime dispersed in 50% W/A solution maintaining the same concentration of 5 g/L. Both products were selected since it has been reported both as the most suitable suspensions in terms of high reactivity assuring a complete carbonation in few hours restoring the binder with a new formed network of calcite crystals [33].

2.3. Nanolime application and samples

In line with a previous work, nanolime of both solutions (water-based nanolime and water + isopropanol-based nanolime) was applied by brush on 6 samples for each testing condition [44]. Consolidant was applied on one face for each cube while the other faces were covered by a thermoplastic film. In 3 of these 6 samples, after consolidant application, a cellulose poultice dipped in distilled water was applied on the treated surface immediately after treatment (Fig. 1c). The poultices were left on the surfaces for 24 h and they were controlled during this time to ensure that each poultice was constantly wet. After each application, the samples were kept under laboratory conditions (15 ± 2 °C and 60 ± 10%RH) during 1 week. In total, 3 applications were performed. Treated samples were left under laboratory conditions (15 ± 2 °C and 60 ± 10% RH) for 2 months prior to testing. Samples impregnated with water-based nanolime were identified as "L" and samples impregnated with water + isopropanol-based nanolime were identified as "LI". For samples where poultices were applied after treatments, a "P" was added to the identifier (ID) following "L" or "LI". In addition, for the 3 unconsolidated samples, which were used as reference, "S" was used as ID.

2.4. Analytical techniques

2.4.1. Preliminary nanolime characterization

In order to have a preliminary evaluation before the treatments of both of the nanolime solutions (in water and in water + isopropanol), firstly 1 mL from both solutions was deposited with a pipette in a watch glass and kept under laboratory conditions (15 ± 2 °C and 60 ± 10%RH) during 1 week. After a careful examination by naked eye, a small amount of dry powder of each of the dry solutions was analysed by means of x-ray powder diffraction (XRD) to know the mineralogical composition using a Siemens D5000. XRD analytical set up conditions were Cu-Kα radiation, Ni filter, 45 kV voltage and 40 mA intensity. Samples were explored in the range between 3 and 60° 2θ with 0.05° 2θ s^{-1} goniometer speed. Each mineral phase was identified using the X'Pert HighScore (Malvern Panalytical B.V.) and its relative abundance (semi-quantitative estimation) was determined using the area of highest-intensity diffraction peaks and the intensity ratios established from artificial mixtures of standard minerals [46]. After that, both dry samples were visualized with a scanning electron microscope (SEM) with energy-dispersive x-ray (EDS) using a FEI Quanta 200 in back-scattered electron (BSE) detection mode. Observation conditions were: a working distance of 9–11 mm, an accelerating potential of 20 kV and a specimen current of ~60 mA.

2.4.2. Uptake, dry matter and retained matter

After treatment, the uptake of the consolidant after each application and the total uptake were calculated by the difference in weight, expressed in g. The treated samples (after 3 applications) were left to dry under laboratory conditions (15 ± 5 °C and 60 ± 10%RH) until reaching constant weight (2 months). At that point, the content of dry matter was determined by difference of weight between the dried treated samples and the samples before consolidation treatment, expressed in g. Moreover, retained matter (dry matter/uptake ratio) in % (w/w) was determined.

2.4.3. Effectiveness of the consolidation treatments

Apparent density (kg/m^3) and open porosity (%) of the reference and the treated samples were determined in accordance with [47] (n = 3 for each testing condition).

Moreover, the porosity and pore size distribution of the samples (reference and treated samples) were determined by mercury intrusion porosimeter (MIP, Micromeritics Autopore III). The fragments of samples (1 cm × 1 cm × 0.5 cm and ~1.5 g) were collected from the first 5 mm beneath the stone surface for analysis. Samples were dried in an oven at 80 °C for 24 h prior to analyses. Two samples were analysed per testing condition.

Superficial cohesion of the reference and the treated samples was evaluated using the peeling test following [48] using the TESA Powerbond double-sided adhesive tape. For each sample three tape strips of 10 mm in width and 40 mm in length were applied and removed consecutively by pulling at an angle of 90°. The peeled off material was determined as the difference between the weight of the tape after removal from the surface and the weight of the tape before application, expressing the results as the mean value of the peeled weight of each surface of the nine strips per each testing condition.

In order to evaluate the consolidation in depth, samples (reference and treated samples) were evaluated using the Drilling Resistance Measurement System (DRMS) from Sint Technology S.r.L and Ultrasounds Pulse Velocity (UPV) measurements. The DRMS was specifically designed to evaluate the efficacy of consolidation treatments in historic mortar and stone substrates [49]. The DRMS measures the force required to drill a hole at constant rotation (rpm) and lateral feed rate (mm/min). It is generally considered the most suitable methodology for quantifying consolidation effectiveness and depth of penetration of consolidants, particularly in soft stones [50–52]. Tests were performed on all testing condition samples using drill bits of 5 mm diameter, a rotation speed of 400 rpm, a rate of penetration of 15 mm/min and a drilling depth of 10 mm (n = 9 per condition).

Ultrasounds Pulse Velocity (UPV) measurements were performed to study differences in the stone's density between the outer part of each sample and its bottom as a result of the consolidation and compared to the unconsolidated reference samples. In order to observe differences in the stone density between the surface and the bottom, measurements were taken by using two positions of the transducers: (1) in perpendicular to the treated face and, (2) in parallel to the treated face (3 depths were evaluated with a separation of approximately of 1 cm). A Panametrics HV Pulser/Receiver 5058 PR coupled with a Tektronix TDS 3012B oscilloscope was used to determine the ultrasound P-wave velocity (v_P) on the samples and data was collected by the lighthouse software. The frequency of Pulse Velocity was constant at 10 MHz. The direct transmission technique was implemented using two pointy transducers (UPE-D), pressed on the opposite ends of the specimens. Velocity is calculated by the following formula: $v_P = L/t$, where v_P is the P-wave velocity (m/s), L is the distance between transducers (m) and t is the time to travel (s). 9 measurements were taken on each of the three samples of each condition and position of the transducers and compared to unconsolidated samples.

2.4.4. Side-effects of the consolidation treatments

Then, side-effects regarding to colour, roughness and hydrophobicity of the stone surfaces were evaluated applying the following techniques:

- Optical microscopy was used by means of a Nikon SMZ800 in order to observe the deposits on the surface inducing chromatic changes.
- Colour of the surfaces was characterized following CIELAB and CIELCH colour spaces [53] using a Minolta CM-700d spectrophotometer. In CIELAB space, L* (lightness), a* and b* (colour coordinates) were measured. L* is the lightness ranging from 0 (absolute black) to 100 (absolute white); a* indicates the colour position between red (positive values) and green (negative values) and b* between yellow (positive values) and blue (negative values). In CIELCH colour spaces, L* is also lightness, C^*_{ab} is the chroma or colour saturation, corresponding to $C^*_{ab} = [(a^*)^2 + (b^*)^2]^{1/2}$ and the h_{ab}, is the hue and is calculated by means of the expression $h_{ab} = \tan [1 - (a^*/b^*)]$. For each specimen, twenty measurements were taken randomly to provide statistically consistent results, being each value the average of three measurements (n = 180 for condition). The measurements were made in the Specular Component Excluded (SCE) mode, for a spot diameter of 3 mm, using the D65 as the illuminant and an observer angle of 10∘. Colorimetric differences were processed as colour differences (ΔL*, Δa*, Δb *, ΔC^*_{ab} and ΔH*) and global colour change (ΔE^*_{ab}) considering as reference the colour of the samples before consolidation [53].
- Profilometry was applied to determine the roughness of each sample using a Mitutoyo SJ400. Following [54], the parameters measured were the arithmetic average roughness (Ra, μm), the root-mean-square roughness (Rq) and the average maximum profile height (Rz, μm). For each testing condition, the equipment traced three scans with a length of 2 cm (n = 9 for each condition).
- Measurement of the static contact angle of the surfaces was taken using a goniometer SEO Phoenix-300 Touch following [55]. The sessile drop method (each drop had 6 μL of deionized water per sample) was applied (n = 9 for testing condition).

Finally, the morphology and distribution within the pores of the calcite crystals originated from the nanolime carbonation were evaluated by a SEM-EDS with the FEI Quanta 200 working with secondary electron (SE) and backscattered electrons (BSE) detectors. Applied optimum conditions of observation were the same as those reported for the nanolime characterization. The specimens were studied by observing the surface directly, and by studying the cross-sections; for this, specimens embedded in epoxy resin (EpoThin 2 Epoxy Resin and EpoThin 2

Epoxy Hardener) then cut and polished to a mirror shine.

3. Results and discussion

3.1. Preliminary nanolime characterization

Observation of the nanolime in both formats on the watch glasses after 2 weeks under laboratory conditions allowed to identify that the dried water-based nanolime formed a continuous layer (Fig. 2a) while the water + isopropanol-based nanolime induced a discontinuous layer on the glass, showing grooves probably caused by the fast evaporation of alcohol (Fig. 2b).

XRD results showed that both nanoconsolidants after 2 weeks under laboratory conditions had a similar composition, but with certain nuances. The water-based nanolime was formed by calcite ($CaCO_3$, 57%) and portlandite ($Ca(OH)_2$, 43%), however the water + isopropanol-based nanolime presented higher content of portlandite ($Ca(OH)_2$, 53%) and it also showed calcite ($CaCO_3$, 37%) and small traces of vaterite ($CaCO_3$, 11%).

SEM allowed the identification of the morphology and composition of the water + isopropanol-based nanolime after drying (Fig. 2c). Few acicular structures were detected, rich in Ca and with S as a minor element (Fig. 2c, EDS1), which were identified as Ca sulphated phases, probably gypsum ($CaSO_4{\cdot}2H_2O$). In addition, calcite ($CaCO_3$) was identified through abundant Ca-rich prisms-shaped crystals (Fig. 2c, EDS2) and plates composed by agglomeration of microscopic Ca-rich prismatic crystals (Fig. 2c, EDS3). Also it was possible to find some spheres corresponding to the vaterite $CaCO_3$ polymorph (Fig. 2c, red arrow).

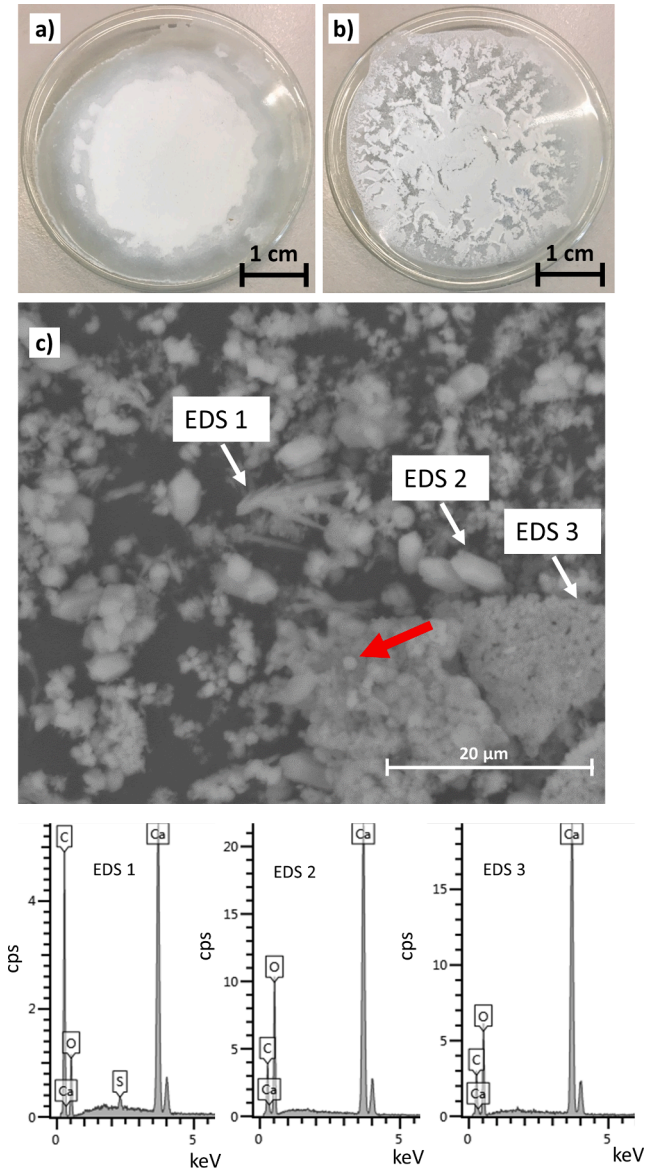

Fig. 2. a) Water-based nanolime and b) water + isopropanol-based nanolime on watch glasses after 2 weeks of drying at laboratory conditions (15 ± 5 °C and 60 ± 10%RH). c) SEM micrograph of water + isopropanol-based nanolime accompanied with 3 EDS spectra. Red arrow shows a vaterite sphere. (For interpretation of the references to color in this figure legend, the reader is referred to the web version of this article.)

3.2. Uptake, dry matter and retained matter.

Regarding the uptake, it was detected that the samples impregnated with the water-based nanolime (L and LP) showed slightly higher values than those for the water + isopropanol-based samples (LI and LIP, Table 1). This fact could be related to the faster evaporation of the isopropanol. In detail, we have detected that:

1) for the samples with water-based nanolime (L and LP), those without cellulose poultice (L) showed lower uptakes than those with poultice (LP). This result was surprising because it should be expected that the contact with the wet poultice during 24 h could have reduced the water absorption of the sample, and then, nanoconsolidant uptake in the second application should be lower. However, the obtained results show us that the uptake is conditioned by the application mode, in this case, by brush (commonly applied by restorer-conservators). This methodology may involve the application of product in excess or in deficiency. Further research should be focus on this very interesting aspect.
2) for the samples with water + isopropanol-based nanolime (LI and LIP), uptakes were similar. For these samples, the application of the wet poultice did not influence on the uptake. This probably happened due to the volatility of the solvent what allowed a faster evaporation and a faster recovery of the water absorption capacity of the stone.

Considering dry matter, similar amounts were obtained for the four conditions (c.a. 0.03 g) although different uptakes were previously determined (higher in the samples with water-based nanolime). Therefore, dry matter seems to be related to the nanolime concentration; although two different solutions were applied (nanolime particles dispersed in water and nanolime dispersed in 50% W/A solution) the same concentration was used (5 g/L). Nevertheless, for the % of retained matter, it has been found that the increase percentage was slightly higher in the samples with water + isopropanol-based nanolime (LI and LIP) regardless of the application of a poultice. It should be related to the faster evaporation of the isopropanol which leads to a reduction of the uptake and consequently a higher retained matter since the dry matter was similar for all the conditions. With respect to those consolidated with water-based nanolime, the samples with poultice (LP) showed lower increase of the retained matter if compared to this nanolime without poultice (L). Once again, the higher retained matter of the L samples seems to be conditioned by the application mode: since the uptake was higher for the LP but the dry matter was similar for both conditions (L and LP), the retained matter has to be lower.

3.3. Effectiveness of the consolidation treatments

The unconsolidated stone (S) showed a total apparent density of 2128.23 ± 28.46 kg/m^3 and a total open porosity of 19.94 ± 0.43% (Table 1), determined in accordance with [47]. However, MIP analysis carried out in the outermost 5 mm showed a higher apparent density

(2556.40 ± 11.20 kg/m^3) and a higher open porosity (27.43 ± 0.30%). Considering the results of the total open porosity for the consolidated stones (Table 1), the apparent density and the open porosity in accordance with [47] did not experience variations since all the values were around 2100 Kg/m^3 and 19–20%, respectively. These results are clearly in line with previous investigations on stone consolidations that suggest that nanolime treatments induce a minimal total open porosity variation after treatments on cubic samples measuring 30 mm × 30 mm × 30 mm [43,56] while noticeable reductions in the open porosity can be only detected by MIP on the superficial 1 cm layer [43]. In the current research, this decrease in the open porosity is certainly noticed by MIP in all impregnated samples in the outer 5 mm of the consolidated samples (Table 1) suggesting that all treatments affected the pore structure of the stone by reducing the modal pore diameter and the porosity. This decrease was also accompanied by a slight increase of apparent density by MIP.

The pore size distributions of control (S) and treated samples are shown in Fig. 3. It can be seen that the control sample has a tri-modal pore size distribution, coarser pores with diameters between 1000 μm and 200 μm, intermediate pores with diameters between 80 μm and 10 μm and finer pores with diameters between 0.5 μm and 0.02 μm (Fig. 3a). Following the treatments, a noticeable reduction of the porosity is noticeable in the cumulative pore volume intrusion in all samples. Consolidated samples present a higher reduction in the finer pores with diameters between 0.5 μm and 0.02 μm and a significant enhancement of the intermediate mode can be observed (Fig. 3b-d), which is associated to the reduction of coarser pores (>1000 μm) outside of the measurement range of the used MIP technique.

The superficial cohesion of the surface was evaluated by peeling test and the results are shown in Fig. 4. It was found that all the treatments induced an increase of the surface cohesion after treatment, which is shown by a decrease of the material peeled off. This decrease was more significant in the samples impregnated with water-based nanolime (L and LP) than those detected in the samples impregnated with water +

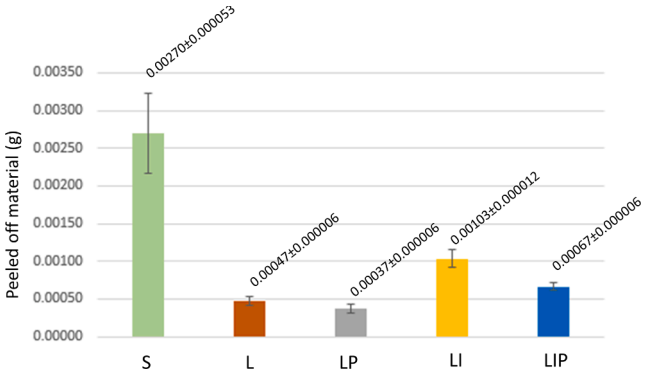

Fig. 4. Results of the peeling test. The values shown are the average amounts of loose (peeled off) matter (expressed by weight in g) stripped from the stone surface by 3 tapes (n = 9 for each testing condition). S is the unconsolidated sample; L is the stone impregnated with water-based nanolime; LI is the stone impregnated with water + isopropanol-based nanolime. LP and LIP are those stones where wet cellulose poultices were applied after the respective treatments.

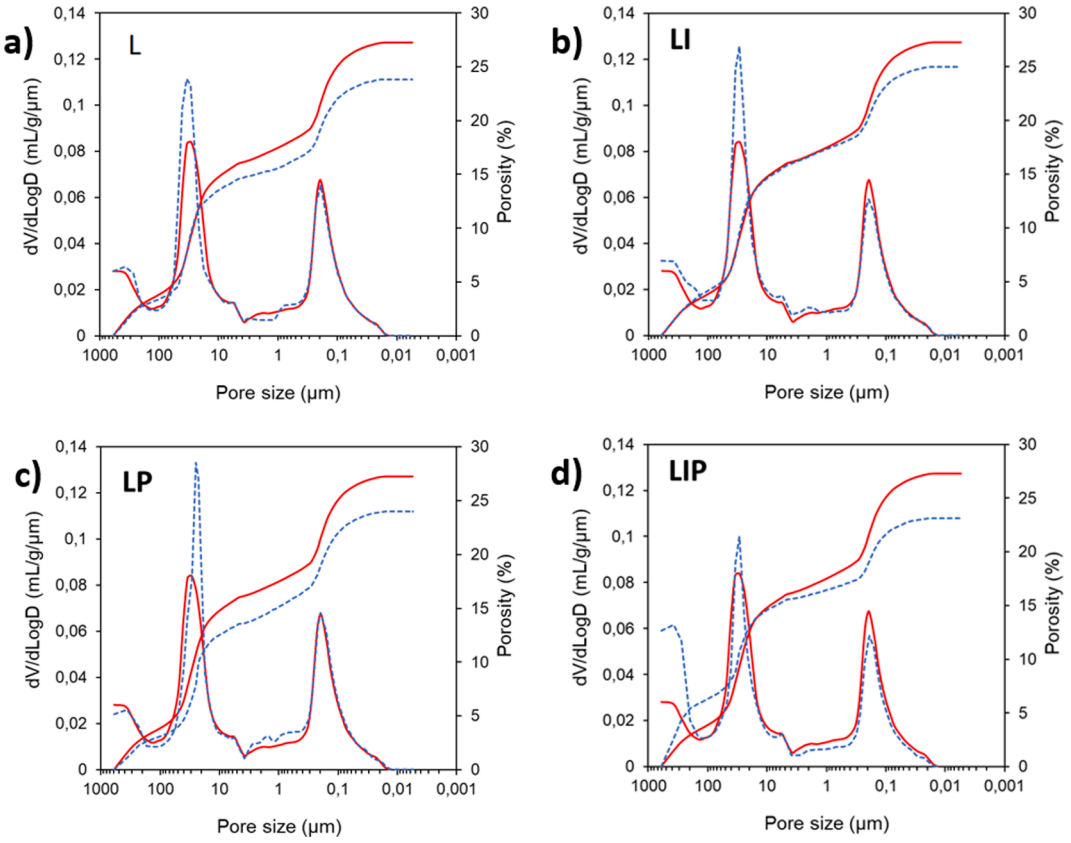

Fig. 3. Log differential intrusion (mL/g) and cumulative pore volume intrusion *versus* pore size diameter (μm) measured by the Mercury Intrusion Porosimeter (MIP). a) Stone impregnated with water-based nanolime (L). b) Stone impregnated with water + isopropanol-based nanolime (LI). c and d) Stones where wet cellulose poultices were applied after the respective treatment (LP and LIP respectively). For each graph, red line corresponds to the results obtained for the unconsolidated sample (S). Blue line corresponds to the results obtained for the impregnated samples. Dotted line corresponds to the cumulative pore volume intrusion. MIP analysis carried out in the first 5 mm beneath the stone surface. (For interpretation of the references to color in this figure legend, the reader is referred to the web version of this article.)

isopropanol-based nanolime (LI and LIP). However, while the poultice application did not induce significant differences for the water-based nanolime samples (L and LP), the poultice showed an increase of the superficial cohesion for the samples with water + isopropanol-based nanolime (LI and LIP) because less amount of material was peeled off from the sample with poultice (LIP). Therefore, the treatments which gave the most significant increase of cohesion of the surface were those with water-based nanolime.

With respect to the drilling resistance (Fig. 5) obtained for the treated samples (blue lines in Fig. 5) in comparison with to the unconsolidated sample (red lines in Fig. 5), it was observed that the water + isopropanol -based nanolime (Fig. 5b) induced higher increase in the resistance than the water-based nanolime (Fig. 5a) throughout the entire evaluated depth (10 mm), as also detected in previous researches [59,60]. On contrary, DRMS results also suggest that the poultice application induced changes in the resistance obtained in comparison with the samples without poultice: i) when poultice was applied after water-based nanolime (Fig. 5c), a resistance increase in the first 1 mm of depth was detected and ii) when poultice was applied after water + isopropanol-based nanolime (Fig. 5d), also a slight increase of the resistance was detected through depth in the first 2 mm. In addition, the increase in the mechanical properties of the samples without poultice (L and LI) was higher compared to the same testing conditions with poultice (LP and LIP). As was reported before, samples without poultice (L and LI) showed a greater peeled off material in comparison to samples with it (LP and LIP). Therefore, samples with higher resistance (higher penetration of the consolidant, L and LI) showed also higher accumulation of product on the surface, which was dragged during the peeling test resulting in a higher peeled off material amount.

The v_P results are shown in Fig. 6. Considering the v_p obtained by placing one of the transducers in the face where the nanolime was applied (v_p located on the upper face of each sample in Fig. 6), an increase in P-wave speed was observed in all the samples (L, LP and LI) with the exception of the sample with water + isopropanol-based nanolime and a poultice (LIP), whose mean v_P was 741.6 ± 25.2 m/s (Fig. 6e) which was statistically similar to that of the unconsolidated stone (S) with v_P of 762.9 ± 41.2 m/s (Fig. 6a). These v_P increases indicate that the impregnated samples present fewer voids in the form of pores, fissures or cavities compared to the unconsolidated sample (S, Fig. 6a) suggesting these specimens were consolidated. This confirms the resistance increase in depth for the treated samples L, LP and LI detected by the DRMS. The absence of P-wave speed increase for the sample with

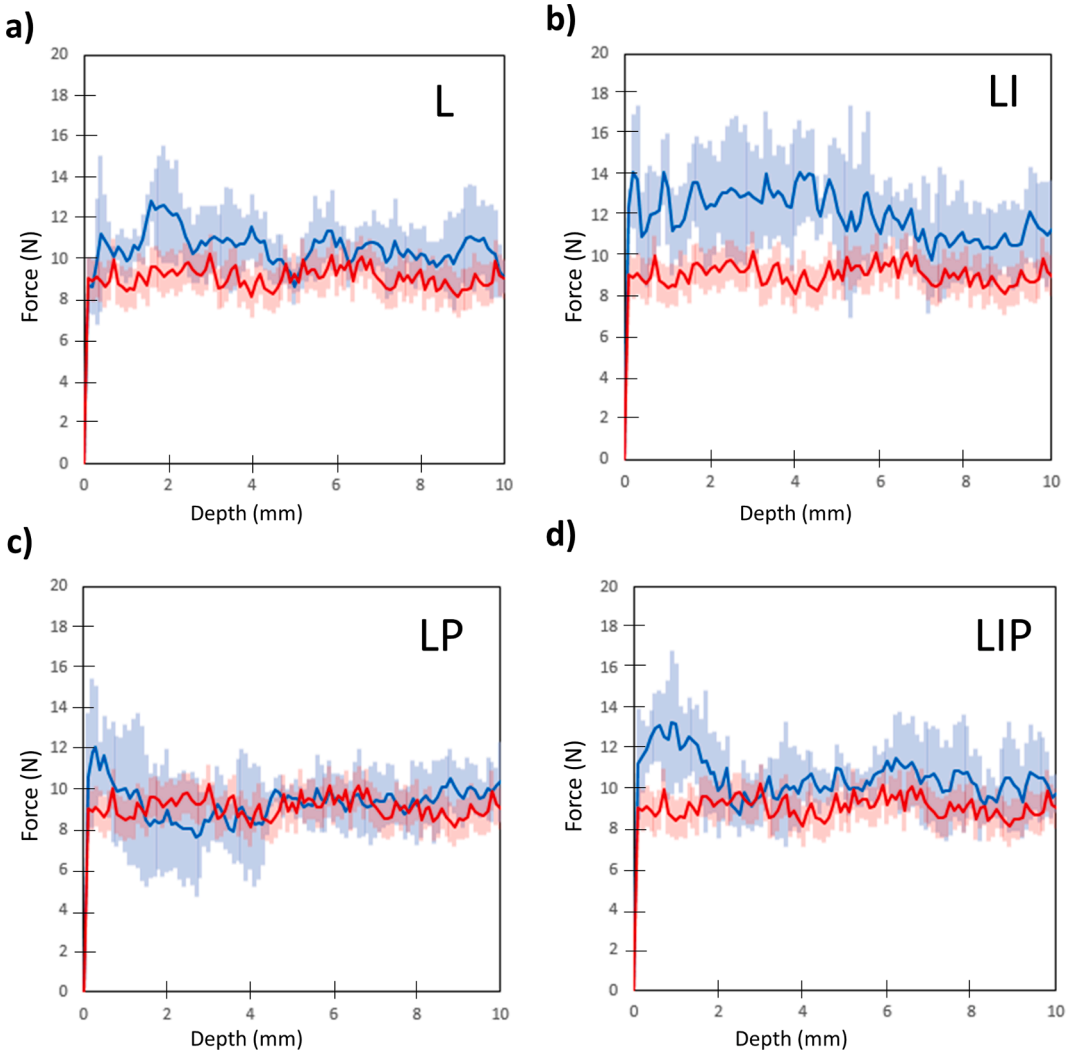

Fig. 5. Force (N) through depth of the sample measured by the Drilling Resistance Measurement System (DRMS). a) stone impregnated with water-based nanolime (L). b) Stone impregnated with water + isopropanol-based nanolime (LI). c and d) Stones where wet cellulose poultices were applied after the respective treatment (LP and LIP respectively). For each graph, red line corresponds to the results obtained for the unconsolidated sample (S). Blue line corresponds to the results obtained for the impregnated samples. Blue and red bars correspond to the standard deviations measured. (For interpretation of the references to color in this figure legend, the reader is referred to the web version of this article.)

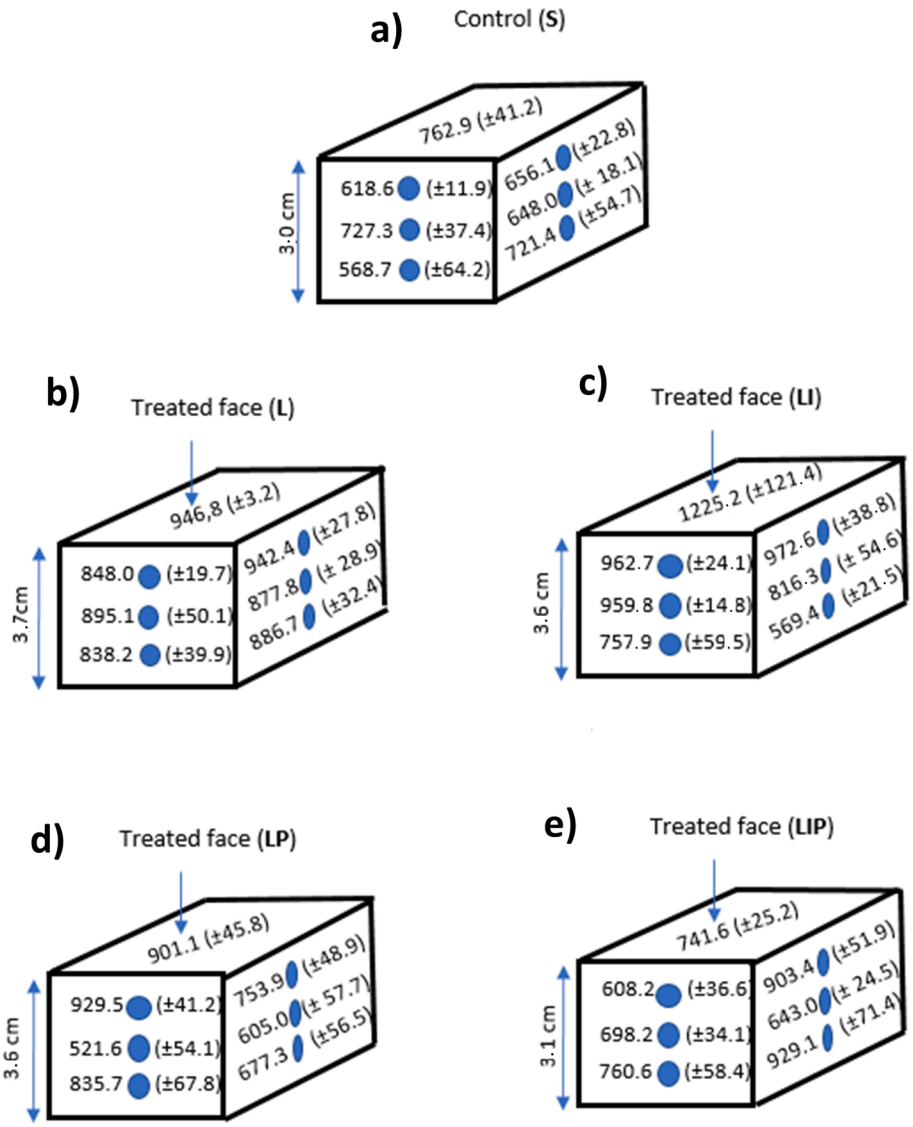

Fig. 6. P wave velocity (v_P, m/s) by ultrasounds test through samples. a) Unconsolidated surface (S). b) Stone impregnated with water-based nanolime (L). c) Stone impregnated with water + isopropanol-based nanolime (LI). d and e) Stones where wet cellulose poultices were applied after the respective treatment (LP and LIP respectively).

the water + isopropanol-based nanolime and a poultice (LIP) can be related to the resistance increase detected by DRMS just in the uppermost 2 mm. The sample with water + isopropanol- based nanolime (without poultice, LI) showed the highest value of v_P (1225.2 ± 121.4 m/s), suggesting the most intense consolidation degree (Fig. 6c).

Attending to the application of the poultice, comparing with the values detected on the samples without poultices, v_P were lower; considering the standard deviations, samples with water-based nanolime (LP) presented similar v_P to those without poultice-L- (901.1 ± 45.8 m/s and 946.8 ± 3.2 m/s respectively, Fig. 6d and b respectively).

The in-depth study allowed the identification of, in general terms, higher v_P in treated face of the samples, up to a depth of 1 cm. In the sample with the highest v_P (water + isopropanol-based nanolime-LI-) higher v_P values were observed up to approximately 2 cm depth comparatively to the reference sample-S- (Fig. 6c and a respectively). Although DRMS was only applied with a drilling depth of 10 mm, the results for the samples with water-based nanolime-L- and water + isopropanol-based nanolime-LI- confirmed the resistance increase due to the filling of pores, fissures or cavities up to this drilling depth.

3.4. Side effects of the consolidation treatments

Stereomicroscopy allowed the identification of the nanolime accumulation on the surface of the limestone (Fig. 7). The surface impregnated with water + isopropanol -based nanolime (LI) presented the highest accumulation of consolidant on the surface (Fig. 7c). These accumulations were dense without cracks (Fig. 7c). However, it was observed that in the sample with this nanolime after poultice application (LIP), nanoconsolidant accumulations showed some superficial cracks (indicated with red arrows in Fig. 7d).

Table 2 shows the values L*, a*, b*, C^*_{ab} and h_{ab} and their corresponding variations (ΔL*, Δa*, Δb*, ΔC^*_{ab} and ΔH*) and the global colour change (ΔE^*_{ab}), considering as colour reference that measured in each sample before consolidant treatment. The most affected parameter corresponds to the L*, showing increases. This confirms that the surfaces after the application of the nanolime showed an undesired surface white veiling if comparing with the original surface. The sample with the highest increase in L* was the sample with water + isopropanol-based nanolime (LI) followed by L, LIP and LP. Therefore, the samples without poultices (L and LI) showed greater L* increases compared with their counterparts with poultice (LP and LIP respectively). The next

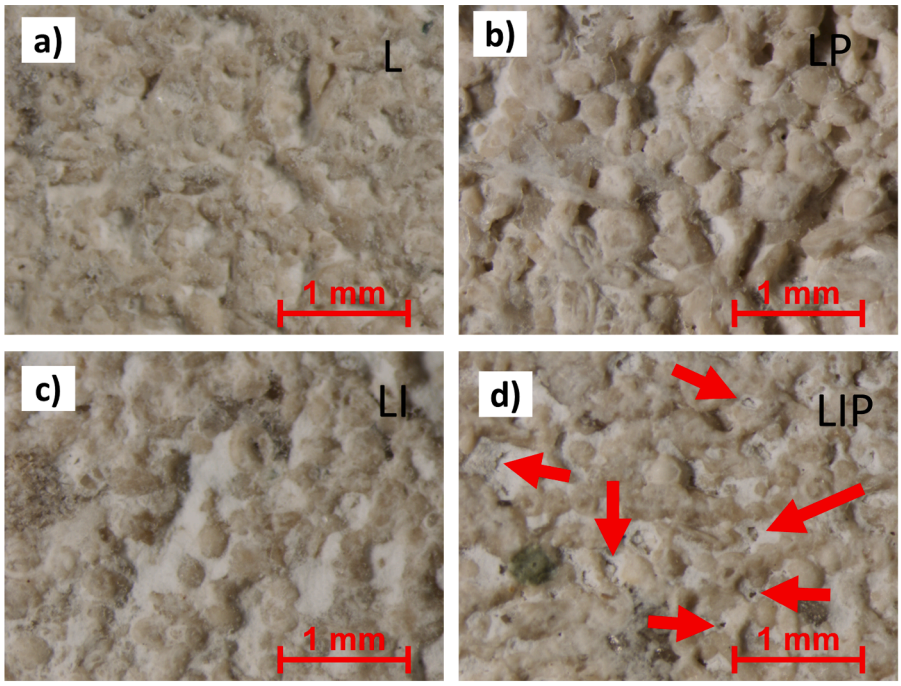

Fig. 7. Micrographs taken with stereomicroscopy of the consolidated stones. a) Stone impregnated with water-based nanolime (L). b) Stone impregnated with water-based nanolime and a wet cellulose poultice (LP). c) Stone impregnated with water + isopropanol-based nanolime (LI). d) Stone impregnated with water + isopropanol-based nanolime and a wet cellulose poultice (LIP). Red arrows point out superficial cracks on the consolidated layer. (For interpretation of the references to color in this figure legend, the reader is referred to the web version of this article.)

Table 2
L*, a*, b*, C^*_{ab} and h_{ab} of the samples: S- unconsolidated stone-, L-stone with water-based nanolime-; LP- stone with water-based nanolime and poultice, LI: stone with water + isopropanol- based nanolime, LIP- stone with water + isopropanol- based nanolime and poultice-. Moreover, changes of theses parameters and global colour change (ΔE^*_{ab}) considering as the reference colour that of the same samples before to be consolidated (n = 180 for condition).

ID	L*	a*	b*	C^*_{ab}	h_{ab}	
S	77.67 ± 2.55	2.31 ± 0.47	11.44 ± 1.66	11.67 ± 1.71	78.66 ± 0.75	
L	80.07 ± 1.09	1.78 ± 0.14	9.12 ± 0.57	9.29 ± 0.58	78.99 ± 0.52	
LP	79.29 ± 1.23	1.96 ± 0.21	10.00 ± 0.70	10.19 ± 0.72	78.93 ± 0.46	
LI	81.26 ± 1.50	1.67 ± 0.21	8.39 ± 0.97	8.56 ± 0.99	78.77 ± 0.36	
LIP	79.79 ± 1.74	1.81 ± 0.36	9.63 ± 1.60	9.80 ± 1.63	79.38 ± 0.51	
ID	ΔL*	Δa*	Δb*	ΔC^*_{ab}	ΔH*	ΔE^*_{ab}
L	2.40	−0.53	−2.32	−2.38	−0.03	3.38
LP	1.62	−0.35	−1.44	−1.49	0.08	2.20
LI	3.59	−0.64	−3.05	−3.11	0.00	4.75
LIP	2.11	−0.50	−1.81	−1.87	0.00	2.82

colorimetric parameter that was affected by the application of the nanolime was b* (decreasing), with the same distribution found for L*. Decreases in b* suggest a loss of yellow coloration. Both the L* increase and the b* reduction are related to the white deposits found filling stone voids. However, a* experimented low decreases (Table 2). As a result of these modifications, C^*_{ab} also underwent changes, specifically decreasing colour intensity. The tone (h_{ab}) hardly suffered modifications.

The sample that experienced the most intense ΔE^*_{ab} was that with water + isoproponal-based nanolime (LI) with a value of 4.75 CIELAB units. Therefore, as ΔE^*_{ab} is greater than 3.5 CIELAB units, this chromatic change should be visible by an inexperienced observer [57]. In the rest of the samples, the ΔE^*_{ab} were less than 3.5 CIELAB units; then, the nanolime does not lead to a visible chromatic change.

It is important to indicate that comparing between samples with water-based nanolime and those with water + isopropanol-based nanolime, the second group showed higher ΔE^*_{ab}. In addition, samples without poultice (L and LI) showed higher ΔE^*_{ab} than those measured in the samples with poultice (LP and LIP).

Considering the wettability of the surfaces (Fig. 8a), it was identified

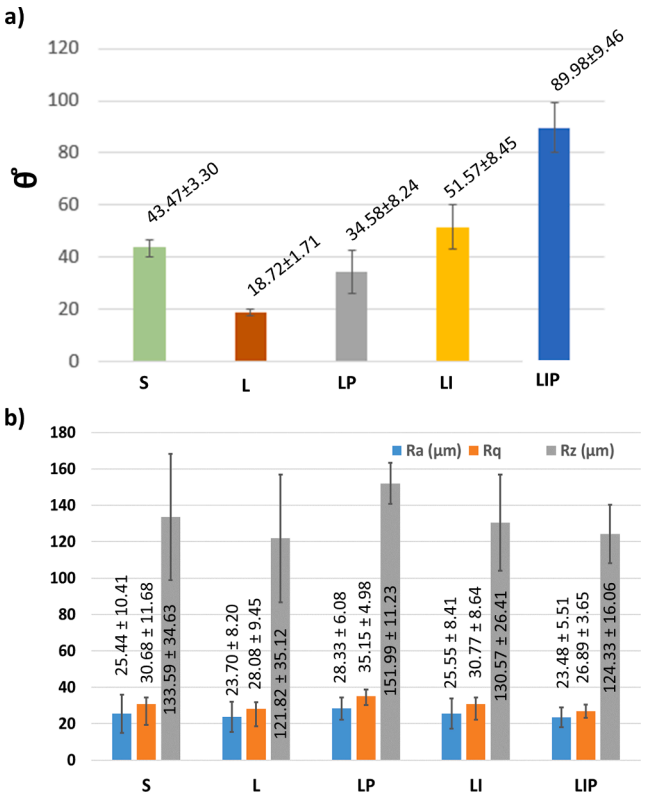

Fig. 8. Results of the static contact angle -θ- (a) and the roughness -Ra, Rq and Rz- (b). S is the unconsolidated sample; L is the stone impregnated with water-based nanolime; LI is the stone impregnated with water + isopropanol-based nanolime. LP and LIP are the samples where wet cellulose poultices were applied after the respective treatment.

that the application of the water + isopropanol-based nanolime followed by a poultice (LIP) was the only condition that led to static contact angles (θ) greater than those measured for the unconsolidated sample (S) (Fig. 8a). The θ of LIP was very close to 90°, which is the value from which a surface is considered hydrophobic [58]. In comparison to the θ of the unconsolidated sample (S), the greatest reduction in the θ was identified on the surface where water-based nanolime (L) was applied. On one hand, comparing samples consolidated with water-based nanolime (L and LP) and those with water + isopropanol-based nanolime (LI and LIP), the former presented the greatest reduction of θ. On the other hand, the samples with poultice (LP and LIP) showed higher θ than their counterparts without poultice (L and LI).

Regarding roughness (Fig. 8b), the three parameters (Ra, Rq and Rz) showed similar trends and taking into account the standard deviations, there were no significant differences between the unconsolidated samples (S) and the 4 conditions (S, L, LP, LI and LIP). However, it was observed that on the surfaces with the water-based nanolime (L) and those with water + isopropanol-based nanolime and poultice (LIP), the roughness parameters were slightly lower than those corresponding to the reference sample (S).

Observations of the surfaces by means of SEM-EDS allowed the identification of accumulation of deposits rich in Ca, C and O and as minor elements S, Cl and S on the surfaces treated with the four conditions (Fig. 9). On the samples treated with both nanolime solutions without poultice (L: Fig. 9a and LI: Fig. 9c), and on that with water-based nanolime and poultice (LP: Fig. 9b), surface accumulations were composed mainly of granular deposits and some plates of calcite while on the surface where poultice was applied after water + isopropanol-based nanolime (LIP, Fig. 9d), a continuous and severely fractured layer was found on the surface (Fig. 9b). SEM observations of the cross-sections also allowed the identification of precipitated calcite accumulated mainly on the surfaces and into the superficial fissures and voids (pointed out with red arrow in Fig. 10).

Therefore, regarding the effect of the medium used with the nanolime (water or 50% v/v of water and isopropanol) and the poultice application on the different physical properties of the stone surfaces evaluated in this research, roughness parameters did not show statistically significant differences in comparison to the reference samples, however different effects were detected for the hydrophobicity and the color. Considering the hydrophobicity, despite to show some fractures, the continuous layer composed by calcite grains on the surface with water + isopropanol-based nanolime and poultice (LIP) detected by SEM, seems to be the reason for the highest static contact angle close to 90° (value from which the surface can be considered hydrophobic). The nanometric roughness generated as result of the fractures developed in the layer could be the reason of this static contact angle increase; this nanometric scale is the specific functional requirement to create a hydrophobic surface [61,62]. The rest of the surfaces (L, LP and LI) showed static contact angles equal or lower than those of the reference samples (S). In those surfaces, calcite grains did not form an external continuous layer but they were accumulated into pores and cracks.

Regarding, color the highest ΔE^*_{ab} on the surfaces with water-based nanolime (LI) was assigned to the greatest calcite accumulation on the surface. The poultice application induced lower ΔE^*_{ab} than the treatments without it, probably due to the highest removal of nanoconsolidant once the poultices were dried and/or extracted, as confirmed by the tiny fractures in the external layer.

4. Conclusions

Results of this preliminary research show that, contrary to what was commonly believed in the practice, the samples where a wet cellulose poultice was applied immediately after the nanolime treatment reached the lowest levels of penetration and, retained lower dry matter in comparison to their counterpart treatments without poultice. Specific results showed that the two nanolime solutions (a water-based

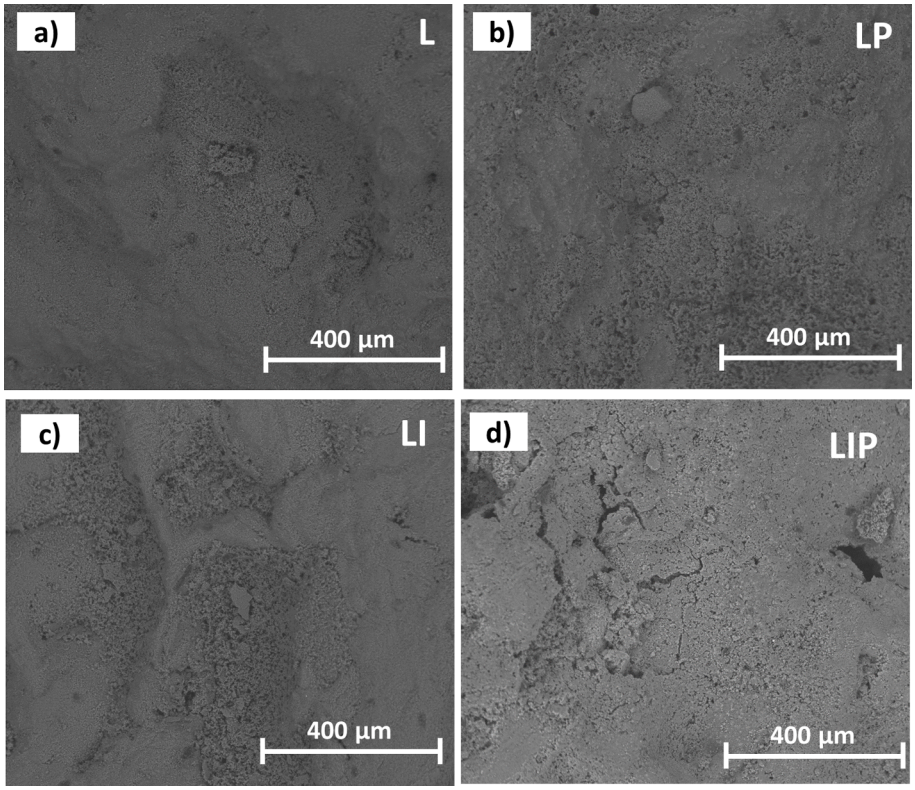

Fig. 9. Micrographs taken with SEM of the surfaces of the treated stones. a) Stone impregnated with water-based nanolime (L). b) Stone impregnated with water-based nanolime and a wet cellulose poultice (LP). c) Stone impregnated with water + isopropanol-based nanolime (LI). d) Stone impregnated with water + isopropanol-based nanolime and a wet cellulose poultice (LIP).

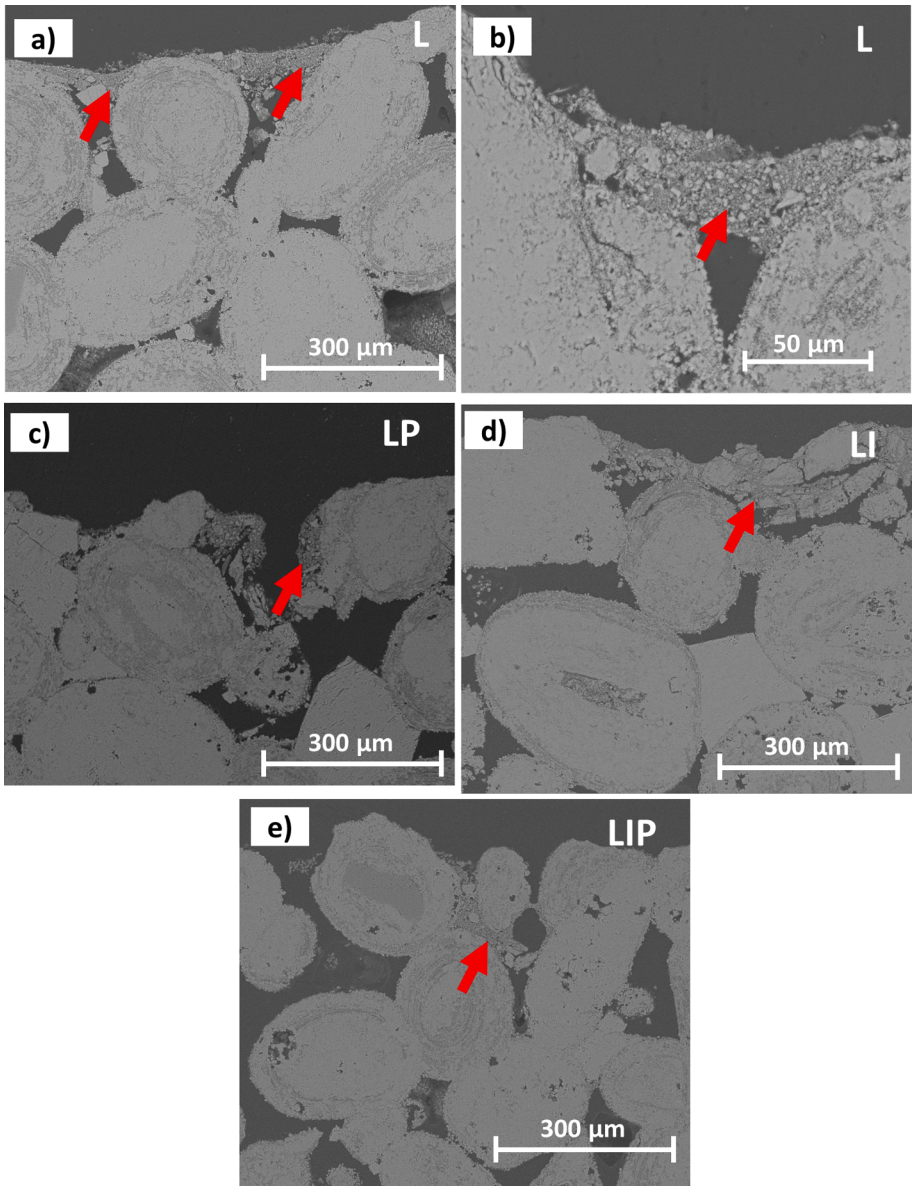

Fig. 10. Micrographs taken with SEM of the cross-sections of the treated stones. a, b) Stone impregnated with water-based nanolime (L). c) Stone impregnated with water-based nanolime and a wet cellulose poultice (LP). d) Stone impregnated with water + isopropanol-based nanolime (LI). e) Stone impregnated with water + isopropanol-based nanolime and a wet cellulose poultice (LIP). Red arrows point out precipitated calcite accumulations. (For interpretation of the references to color in this figure legend, the reader is referred to the web version of this article.)

dispersion and a water + isopropanol at 50% v/v -based solution) achieved a clear reduction in the open porosity in the outer 5 mm of the sample increasing both the internal mechanical properties of the samples (obtaining a consolidating effect in up to 1 cm in-depth) while also increasing its surface cohesion. The two nanolime solutions with a poultice seemed to achieved a less pronounced increase in the mechanical properties determined by DRMS, lower reduction of the open porosity, lower penetration and lower surface cohesion. However, both treatments with nanolime without poultices showed higher levels of accumulation of calcite-rich deposits on the surfaces which were visually identifiable and clearly recorded by the spectrophotometer. This is clearly in the line with the practice observations that suggest that the use of poultices reduces the appearance of the white veiling on the surface.

Further research will concern an in-depth study on the effect of poultices on the consolidation of commercial nanolime products. These results also suggest that a consolidation treatment with nanolime is more complex that it is generally assumed, and the application of poultices is not always simply enhancing consolidation degree; the most suitable application procedure must be chosen with regards to the nanolime and substrate specific characteristics. The results reported in this article would help conservation practitioners when making decisions regarding interventions directly in built heritage buildings with this type of limestone.

CRediT authorship contribution statement

J.S. Pozo-Antonio: Conceptualization, Investigation, Resources, Methodology, Software, Data curation, Supervision, Project administration, Writing – original draft, Writing – review & editing, Funding acquisition. **J. Otero:** Conceptualization, Investigation, Resources, Methodology, Software, Data curation, Visualization, Supervision, Project administration, Writing – review & editing, Funding acquisition. **N. González:** Investigation, Methodology, Software, Data curation.

Declaration of Competing Interest

The authors declare that they have no known competing financial interests or personal relationships that could have appeared to influence the work reported in this paper.

Acknowledgments

J.S. Pozo-Antonio was supported by the Ministry of Science and Innovation, Government of Spain through grant number RYC2020-028902-I. J. Otero's current research is funded by the European Commission on the Marie Skłodowska-Curie Actions (MSCA-IF) from the European Union's Horizon 2020 on research and innovation, grant agreement N. 893762 (NANOMORT). Funding for open access charge was provided by Universidade de Vigo/CISUG.

References

[1] E. Doehne, C.A. Price, Stone conservation: an overview of current research, Research in conservation series. Getty Conservation Institute, Los Angeles, 2009.
[2] B. Silva, T. Rivas, B. Prieto, Soluble Salts in Granitic Monuments: Origin and Decay Effects, ASTM American Society of Testing Materials, 2003, pp. 113–130.
[3] L. Lazzarini, M.L. Tabasso, Il restauro della pietra, CEDAM-Casa Editrice Dott. A, Milani, 1986.
[4] R. Esbert, M. Montoto, J. Ordaz, La piedra como material de construcción: durabilidad, deterioro y conservación, Materiales de construcción 41 (1991) 221.
[5] R.M. Esbert, J. Ordaz, F.J. Alonso, M. Montoto, Manual de diagnosis y tratamiento de materiales pétreos y cerámicos. Colegio de aparejadores y arquitectos técnicos de Barcelona. 1ª Edición. ISBN: 84-87104-29-0. 1997.
[6] J.S. Pozo-Antonio, T. Rivas, M.P. Fiorucci, A. Ramil, A.J. López, Effectiveness of granite cleaning procedures in cultural heritage: a review, Sci. Total Environ. 571 (2016) 1017–1028.
[7] ICOMOS-ISCS. Illustrated glosary on Stone deterioration patterns. Monuments ans Sites: XV. 78 pages. ISBN: 978-2-918086-00-0. 2008.
[8] B. Hermosin Campos, Efectos de la contaminación atmosférica sobre el patrimonio histórico. Deposición de compuestos orgánicos y formación de costras negras sulfatadas, Tesis doctoral, Facultas de Química. Universidad de Sevilla, 1995.
[9] J. Watt, J. Tidblad, V. Kucera, R. Hamilton, The effects of air pollution on cultural heritage. Springer. 306 pages. ISBN: 978-0-387-84892-1. 2009.
[10] MDCS (Monument Diagnosis and Conservation System), The online damage-expert for monumental buildings https://mdcs.monumentenkennis.nl/damageatlas/4/material.
[11] W.H. Dukes, Coservation os stone: chemical treatments, Architectś J Inf Library (1972) 433-438.
[12] W.H. Gutt, Conservation of Stone. The Next Steps. London. Stone industries. 1973.
[13] J.R. Clifton, G.J.C. Frohnsdorff, Stone-Consolidating Materials: A Status Report. Conservation of Historic Stone Buildings and Monuments (1982) 287-311.
[14] C. Price, K. Ross, G. White, A further appraisal of the 'Lime Technique' for limestone consolidation, using a radioactive tracer, IIC J Stud Conserv 33 (4) (1988) 178–186.
[15] I. Brajer, N. Kalsbeek, Limewater absorption and calcite crystal formation on a limewater-impregnated secco wall-painting, Stud. Conserv. 44 (3) (1999) 145–156.
[16] C. Rodriguez-Navarro, E. Ruiz-Agudo, Nanolimes: from synthesis to application, Pure Appl. Chem. 90 (3) (2018) 523–550.
[17] M.J. Mosquera, J. Pozo, L. Esquivias, Stress during drying of two stone consolidants applied in monumental conservation, J. Sol-Gel Sci. Technol. 26 (2003) 1227–1231.
[18] G. Wheeler, Alkoxysilanes and consolidation of stone, Research in conservation Series. Getty Conservation Institute, Los Angeles, 2005.
[19] C. Salazar-Hernandez, R. Zarraga, S. Alonso, S. Sugita, S. Calixto, J. Cervantes, Effect of solvent type on polycondensation of TEOS catalysed by DBTL as used for Stone consolidation, J. Sol-Gel Sci. Technol. 49 (2009) 301–310.
[20] J.S. Pozo-Antonio, J. Otero, P. Alonso, X. Mas i Barberà, Nanolime and nanosilica-based consolidants applied on heated granite and limestone: effectiveness and durability Constr. Build. Mater. 201 (20) (2019) 852-870.
[21] G.A. Ozin, A.C. Arsenault, Nanochemistry, RSC Publishing, Cambridge, 2005.
[22] R. Miranda, Efectos de cuántico y su importancia para la reactividad y estabilidad de nanoestructuras, Revista Sistema madri+d, Especial Nonociencia y Nanotecnología. Monografía 15 (2006) 19–25.
[23] S. Sequeira, C. Casanova, E.J. Cabrita, Deacidification of paper using dispersions of Ca(OH)2 nanoparticles in isopropanol, J Cult Herit 7 (2006) 264–272.
[24] I. Berlanga Mora, Síntesis y caracterización de nanomateriales 0D, 1D y 2D. Tesis Doctoral. Universidad Autónoma de Madrid. Facultad de Ciencias. Departamento de Química Inorgánica. 2013.
[25] V. Daniele, G. Taglieri, R. Quaresima, The nanolimes in cultural heritage conservation: characterisation and analysis of the carbonatation process, J Cult Herit 9 (3) (2008) 294–301.
[26] P. Baglioni, D. Chelazzi, R. Giorgi, E. Carretti, N. Toccafondi, Y. Jaidar, Commercial $Ca(OH)_2$ nanoparticles for the consolidation of immovable works of art, Appl. Phys. A Mater. Sci. Process. 114 (3) (2014) 723–732.
[27] P. Baglioni, D. Chelazzi, R. Giorgi, Nanotechnologies in the Conservation of Cultural Heritage: A Compendium of Materials and Techniques, Springer, New York, 2015.
[28] J. Otero, A.E. Charola, C.A. Grissom, V. Starinieri, An overview of nanolime as a consolidation method for calcareous substrates, GE Conserv. 1 (11) (2017) 71–78.
[29] L. Dei, B. Salvadori, Nanotechnology in cultural heritage conservation: nanometric slaked lime saves architectonic and artistic surfaces from decay, J Cult Herit 7 (2) (2006) 110–115.
[30] A. Sierra-Fernandez, L.S. Gomez-Villalba, M.E. Rabanal, R. Fort, New nanomaterials for applications in conservation and restoration of stony materials: a review. Materiales de Construcción 67, (325) (2017).e107.
[31] G. Taglieri, V. Daniele, D. Re, et al., A new and original method to produce Ca $(OH)_2$ nanoparticles by using an anion exchange resin, Adv. Nanopart. 4 (2015) 17–24.
[32] G. Taglieri, B. Felice, V., Daniele et al., Analysis of the carbonisation process of nanosized $Ca(OH)_2$ particles synthesized by exchange ion process. Proceedings of the Institution of Mechanical Engineers, Part N: Journal of Nanoengineering and Nanosystems 230 (1) (2016), 25-31.
[33] G. Taglieri, V. Daniele, L. Macera, C. Mondelli, Nano $Ca(OH)_2$ synthesis using a cost-effective and innovative method: Reactivity study, J.Am Ceram Soc. 100 (12) (2017) 5766–5778.
[34] L.S. Gómez-Villalba, P. López Arce, M. Alvarez de Buergo, R. Fort, Structural stability of a colloidal solution of $Ca(OH)_2$ nanocrystals exposed to high relative humidity conditions, Appl. Phys. A 104 (2011) 1249–1254.
[35] P. López-Arce, L.S. Gómez-Villalba, L. Pinho, M.E. Fernández-Valle, M. Álvarez de Buergo, R. Fort, Influence of porosity and relative humidity on consolidation of dolostone with calcium hydroxide nanoparticles: effectiveness assessment with non-destructive techniques, Mater. Charact. 61 (2010) 168–184.
[36] E. Hansen, E. Doehne, J. Fidler, J. Larson, B. Martin, M. Metteini, C. Rodríguez-Navarro, E. Sebastián Pardo, C. Price, A. de Tagle, J.M. Teutónico, N. Weiss, A review of selected inorganic consolidants and protective treatment for porous calcareous materials, Rev. Conserv. 4 (2004) 13–25.
[37] G. Borsoi, B. Lubelli, R. van Hees, R. Veiga, A.S. Silva, Understanding the transport of nanolime consolidants within Maastricht limestone, J. Cult. Heritage 18 (2016) 242–249.
[38] G. Borsoi, B. Lubelli, R. Van Hees et al., Deposition of modified nanolimes within calcareous substrates. 1-2. Abstract from Green Conservation of Cultural Heritage, 27-28 October 2015, Rome, Italy.
[39] G. Borsoi, B. Lubelli, R. Van Hees, et al., Effect of solvent on nanolime transport within limestone: How to improve in-depth deposition, Colloids Surf. A 497 (2016) 171–181.
[40] A. Arizzi, L.S. Gomez-Villalba, P. Lopez-Arce, et al., Lime mortar consolidation with nanostructured calcium hydroxide dispersions: the efficacy of different consolidating products for heritage conservation, Eur J Miner 27 (3) (2015) 311–323.
[41] CTS. Nanorestore. Ficha técnica. Available online: https://shop-espana.ctseurope.com/documentacioncts/fichastecnicasweb2018/2.1consolidantes2016/nanorestoreesp.pdf (accesed on 15dec 2021).
[42] Calosil IP5. Ficha técnica. Available online: https://www.calosil.de/downloads-en (accessed on 15 dec 2021).
[43] J. Otero, V. Starinieri, A.E. Charola, Influence of substrate pore structure and nanolime particle size on the effectiveness of nanolime treatments, Constr. Build. Mater. 209 (2019) 701–708.
[44] J. Otero, J.S. Pozo-Antonio, C. Montojo, Influence of application method and number of applications of nanolime on the effectiveness of the Doulting limestone treatments, Mater. Struct. 54 (2021) 41.
[45] C. Rodriguez-Navarro, I. Bettori, E. Ruiz-Agudo, Kinetics and mechanism of calcium hydroxide conversion into calcium alkoxides: implications in heritage conservation using nanolimes, Langmuir 32 (20) (2016) 5183–5194.
[46] CR. de Kimpe, Clay and silt analysis. In: Carter MR, editor. Soil sampling and methods of analysis. Canadian Society of Soil Science, Lewis Publisher, 1993. p. 719–30. [Chapter 67].
[47] UNE-EN 1936:2006. Natural Stone Test Methods – Determination of Real Density and Apparent Density, and of Total and Open Porosity.
[48] M. Drdácky, J. Lesák, S. Rescie, Z. Slízková, P. Tiano, J. Valach, Standardization of peeling test for assessing the cohesion and consolidation characteristics of historic stone surfaces, Mater. Struct. 45 (2012) 505–520.
[49] D. Costa, J. Delgado-Rodrigues, Consolidation of a porous limestone with nano-lime", in: G. Wheeler (Ed.), 12th International congress on the deterioration and conservation of stone, New York, pp. 10–19. 2012.
[50] P. Tiano, Biodegradation of Cultural Heritage: Decay Mechanisms and Control Methods", CNR-Centro di Studio Sulle Cause Deperimento e Metodi Conservazione Opere d'Arte, 9, (2001), 1–37. Available at: http://www.arcchip.cz/w09/w09_tiano.pdf.
[51] F. Fratini, S. Rescic, P. Tiano, A new portable system for determining the state of conservation of monumental stones, Mater. Struct. J. 39 (2) (2007) 139–147.
[52] A. P. Ferreira-Pinto, and J. Delgado-Rodrigues, Hydroxylating conversion treatment and alkoxysilane coupling agent as pre-treatment for the consolidation of limestones with ethyl silicate. In Stone Consolidation in Cultural Heritage: Research and Practice; Proceedings of the International Symposium, Lisbon, 6-7 May 2008, ed. J. Delgado-Rodriguez and J. M. Mimoso, 41-52. Lisbon: LNEC (Laboratorio National de Engenheria Civil).
[53] CIE S014–4, E:2007. L*a*b* Colour Space, Commission Internationale de l'eclairage. CIE Central Bureau, Vienna.
[54] UNE-EN ISO 4288:1998. Geometrical Product Specifications (GPS). Surface texture: profile method. Rules and procedures for the assessment of surface texture. AENOR, Spain.
[55] BS EN 828:2013. Adhesives. Wettability. Determination by measurement of contact angle and surface free energy of solid surface. European Standards.
[56] S. Tzavellos, G.L. Pesce, L. Wu, A. Henry, S. Robson, R.J. Ball, Effectiveness of nanolime as a stone consolidant: a 4-year study of six common UK limestones, Materials 12 (17) (2019) 2673.
[57] W. Mokrzycki, M. Tatol, Colour difference ΔE—a survey, Mach Graph Vis 20 (2011) 383–411.

[58] J. Bico, U. Thiele, D. Quéré, Wetting of textured surfaces, Colloids Surfaces A Physicochem. Eng. Asp. 206 (1-3) (2002) 41–46.
[59] G. Taglieri, J. Otero, V. Daniele, G. Gioia, L. Macera, V. Satinieri, A.E. Charola, The biocalcarenite stone of Agrigento (Italy): preliminary investigations of compatible nanolime treatments, J. Cult. Heritage 30 (2018) 92–99.
[60] J. Otero, V. Sarinieri, A.E. Charola, G. Taglieri, Influence of different types of solvent on the effectiveness of nanolime treatments on highly porous mortar substrates, Constr. Build. Mater., 230, (2020), 117112.
[61] M. Zhang, S. Feng, L. Wang, Y. Zheng, Lotus effect in wetting and self-cleaning, Biotribology 5 (2016) 31–43.
[62] E. Fadeeva, B. Chichkov, E. Fadeeva, B. Chichkov, Biomimetic liquid-repellent surfaces by ultrafast laser processing, Appl. Sci. 8 (2018) 1424.